12. GenBank accession number X73298.
13. B. Baur, K. Fisher, K. Winter, K. J. Dietz, *Plant Physiol.* **106**, 1225 (1994).
14. M. Wada, personal communication.
15. Mutant cDNA sequences were obtained by reverse transcription followed by PCR amplification with total RNAs and *NPH1*-specific primers. PCR products were purified with a QIAGEN PCR purification kit and sequenced directly. Both strands of the entire cDNA sequence for each mutant were examined for mutations, and each lesion was confirmed by two independent PCR experiments.
16. J. P. Khurana and K. L. Poff, *Planta* **178**, 400 (1989).
17. Because *nph1-2* is in the Estland ecotype, we also sequenced an Estland wild-type cDNA for comparison.
18. An additional allele, *nph1-3*, is identical in sequence to *nph1-1*.
19. S. Hill, S. Austin, T. Eydmann, T. Jones, R. Dixon, *Proc. Natl. Acad. Sci. U.S.A.* **93**, 2143 (1996).
20. S. I. Bibikov, R. Biran, K. E. Rudd, J. S. Parkinson, *J. Bacteriol.* **179**, 4075 (1997); A. Rebbapragada *et al.*, *Proc. Natl. Acad. Sci. U.S.A.* **94**, 10541 (1997).
21. W. A. Catterall, *Science* **242**, 50 (1988); J. Tytgat, K. Nakazawa, A. Gross, P. Hess, *J. Biol. Chem.* **268**, 23777 (1993).
22. X. Li, J. Xu, M. Li, *J. Biol. Chem.* **272**, 705 (1997).
23. M. Ahmad and A. R. Cashmore, *Nature* **366**, 162 (1993); C. Lin, M. Ahmad, J. Chan, A. R. Cashmore, *Plant Physiol.* **110**, 1047 (1996).
24. I. B. Zhulin, B. L. Taylor, R. Dixon, *Trends Biochem. Sci.* **22**, 331 (1997); Z. J. Huang, I. Edery, M. Rosbash, *Nature* **364**, 259 (1993).
25. E. Huala *et al.*, data not shown.
26. Single-letter abbreviations for the amino acid residues are as follows: A, Ala; C, Cys; D, Asp; E, Glu; F, Phe; G, Gly; H, His; I, Ile; K, Lys; L, Leu; M, Met; N, Asn; P, Pro; Q, Gln; R, Arg; S, Ser; T, Thr; V, Val; W, Trp; and Y, Tyr.
27. K. Meyer, M. P. Leube, E. Grill, *Science* **264**, 1452 (1994).
28. J. J. Kieber, M. Rothenberg, G. Roman, K. A. Feldmann, J. R. Ecker, *Cell* **72**, 427 (1993).
29. F. Kunst *et al.*, *Nature* **390**, 249 (1997).
30. P. Ballario *et al.*, *EMBO J.* **15**, 1650 (1996).
31. D. Leong, F. Pfeifer, H. W. Boyer, M. C. Betlach, *J. Bacteriol.* **170**, 4903 (1988).
32. J. W. Warmke and B. Ganetzky, *Proc. Natl. Acad. Sci. U.S.A.* **91**, 3438 (1994).
33. J. Ludwig *et al.*, *EMBO J.* **13**, 4451 (1994).
34. T. Kaneko *et al.*, *DNA Res.* **3**, 109 (1996).
35. M. H. Drummond and J. C. Wooton, *Mol. Microbiol.* **1**, 37 (1987).
36. G. Blanco, M. Drummond, P. Woodley, C. Kennedy, *ibid.* **9**, 869 (1993); R. Raina, U. K. Bageshwar, H. K. Das, *Mol. Gen. Genet.* **237**, 400 (1993).
37. D. Siddavattam, H. D. Steibl, R. Kreutzer, W. Klingmuller, *Mol. Gen. Genet.* **249**, 629 (1995).
38. H. Allmeier, B. Cresnar, M. Greck, R. Schmitt, *Gene* **111**, 11 (1992).
39. R. F. Smith and T. E. Smith, *Protein Eng.* **5**, 35 (1992).
40. F. Gropp and M. C. Betlach, *Proc. Natl. Acad. Sci. U.S.A.* **91**, 5475 (1994).
41. F. Narberhaus, H.-S. Lee, R. A. Schmitz, L. He, S. Kustu, *J. Bacteriol.* **177**, 5078 (1995).
42. S. K. Crosthwaite, J. C. Dunlap, J. J. Loros, *Science* **276**, 763 (1997).
43. We thank K. Meyer and W. Lukowitz for providing the genomic library, J. R. Ecker for providing the cDNA and YAC libraries, C. Somerville for assistance with the AFLP technique, and P. Reymond for many helpful comments on the manuscript. This work was funded by NSF grants MCB-9219256 and IBN-9601164. This paper is Carnegie Institution of Washington. Department of Plant Biology publication 1367.

2 September 1997; accepted 5 November 1997

Alignment of Conduits for the Nascent Polypeptide Chain in the Ribosome-Sec61 Complex

Roland Beckmann,* Doryen Bubeck, Robert Grassucci, Pawel Penczek, Adriana Verschoor, Günter Blobel, Joachim Frank

An oligomer of the Sec61 trimeric complex is thought to form the protein-conducting channel for protein transport across the endoplasmic reticulum. A purified yeast Sec61 complex bound to monomeric yeast ribosomes as an oligomer in a saturable fashion. Cryo–electron microscopy of the ribosome-Sec61 complex and a three-dimensional reconstruction showed that the Sec61 oligomer is attached to the large ribosomal subunit by a single connection. Moreover, a funnel-shaped pore in the Sec61 oligomer aligned with the exit of a tunnel traversing the large ribosomal subunit, strongly suggesting that both structures function together in the translocation of proteins across the endoplasmic reticulum membrane.

The existence of a protein-conducting channel (PCC) for protein transport across the endoplasmic reticulum (ER) was proposed in 1975 (*1*). Electrophysiological experiments in 1991 provided the first direct evidence for the existence of the PCC (*2*). Moreover, fluorescently labeled nascent chains in membrane-bound ribosomes remain in an aqueous environment sealed from the cytoplasm and accessible to fluorescence quenching from the lumen of the ER (*3*). An aqueous pore with a diameter of 40 to 60 Å during cotranslational translocation is suggested by similar experiments (*4*).

The Sec61 trimeric complex is a strong candidate for the PCC of the ER in yeast and mammalian cells (*5*, *6*). The Sec61 complex provides the principal binding site for ribosomes at the ER during protein translocation (*7*, *8*) and, together with other membrane proteins, is associated with ribosomes after solubilization of rough microsomes with digitonin (*6*). A two-dimensional map of the purified Sec61 complex obtained by electron microscopy has revealed a quasi-pentagonal, circular structure with a central depression (*9*).

The three-dimensional (3D) structure of monomeric ribosomes is currently known at various resolutions for *Escherichia coli* (*10*), wheat germ (*11*), and yeast (*12*). Among the structural features recognized is a tunnel that traverses the large ribosomal subunit and has been considered a candidate for the nascent chain conduit. Here, we present a 3D reconstruction of the ribosome-Sec61 complex.

For purification of the trimeric Sec61 complex (*13*) containing the Sec61α, Sec61β, and Sec61γ subunits (Sec61p, Sbh1p, and Sss1p), a heptameric complex (*14*) was isolated first with protein A–tagged Sec63 protein, followed by elution of the trimeric Sec61 complex with Triton X-100 (Fig. 1A). To determine whether the trimeric Sec61 complex could bind to ribosomes (*15*) in a membrane-free system, we incubated the purified Sec61 complex with ribosomes and analyzed the incubation mixture by sucrose density-gradient centrifugation (*16*). The Sec61 complex incubated without ribosomes remained in the top fraction of the gradient. In the presence of ribosomes, however, the Sec61 complex migrated with ribosomes as determined by immunoblotting (*16*) with antibodies to Sec61β (anti-Sec61β) (Fig. 1B) and Sec61α (anti-Sec61α) (*17*). In agreement with the known salt sensitivity of the Sec61-ribosome interaction, there was no binding at 1 M KOAc (OAc, acetate) (*17*). Incubation of a fixed amount of ribosomes with increasing amounts of Sec61 complex resulted in saturation of ribosome-binding sites (Fig. 1, C and D). On the basis of the amount of Sec61α and ribosomes, we estimate that, at saturation, two to four Sec61 trimers were bound per ribosome and that the dissociation constant K_d is about 10 nM.

The ribosome-Sec61 complex formed under saturating conditions was examined by cryo–electron microscopy (*18*). In the

R. Beckmann and G. Blobel, Howard Hughes Medical Institute, Laboratory of Cell Biology, Rockefeller University, 1230 York Avenue, New York, NY 10021, USA.
D. Bubeck, R. Grassucci, A. Verschoor, Wadsworth Center, New York State Department of Health, Empire State Plaza, Albany, NY 12201–0509, USA.
P. Penczek and J. Frank, Wadsworth Center, New York State Department of Health, and Department of Biomedical Sciences, State University of New York at Albany, Empire State Plaza, Albany, NY 12201–0509, USA.

*To whom correspondence should be addressed. E-mail: beckmar@rockvax.rockefeller.edu

electron micrographs (Fig. 2A), the ribosome-Sec61 complex appears in random orientations (Fig. 2B). This distribution allowed an artifact-free 3D reconstruction by means of a 3D projection alignment procedure (*19*) with an existing reconstruction of the ribosome from yeast (*12*) as a reference. In side views of the ribosome (marked by arrows in Fig. 2B), an ~100 Å–long ellipsoidal mass of density appears at the surface of the large subunit. This location on the ribosome is the same as the site where, in projection, the exiting polypeptide chain was located on both eubacterial and eukaryotic ribosomes by immuno–electron microscopy (*20*).

In the resulting reconstruction (Fig. 3), which has a resolution of 26 Å (*21*), the Sec61 complex appears as a slightly pentagonally shaped toroidal structure with an outer diameter of 95 Å, an inner diameter ranging from 15 to 35 Å depending on depth, and an overall thickness of 40 Å supported by a single stem attached to the base of the large ribosomal subunit. A single site of rigid attachment may facilitate lateral opening of the channel, at the opposite site, to allow the release of nascent transmembrane segments into the lipid bilayer. The surface of the Sec61 oligomer facing the ribosome is parallel to the surface of the large subunit. The distance between these surfaces ranges from 15 to 20 Å. Hence, the attachment of the Sec61 oligomer to the ribosome does not appear to form the tight seal that was implicated in nascent chain fluorescence-quenching experiments. Seal-forming proteins could be missing, or, more likely, the signal sequence may be necessary for seal formation (*2*, *3*, *8*, *22*).

The central pore of the Sec61 oligomer aligns precisely with an opening in the large ribosomal subunit that represents the exit of a tunnel (Fig. 3B). This tunnel runs from the interface canyon (*12*) to the lower portion of the large subunit (Fig. 3D). At the threshold level chosen (*23*), a small segment of the tunnel is blocked because of the limiting resolution, but it appeared to be open at increased threshold levels (*17*). A similar effect has been observed in the reconstruction of the 70S *E. coli* ribosome (*10*). These tunnels, seen in cryo–electron microscopy maps of the ribosome from *E. coli* (*10*) and *Saccharomyces cerevisiae* (*12*),

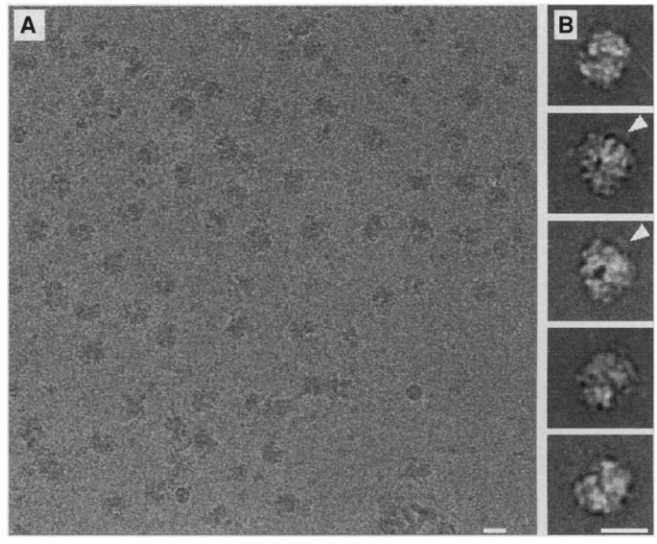

Fig. 2. (**A**) Cryo–electron micrograph showing a field of yeast ribosome-Sec61 complexes. Scale bar, 200 Å. (**B**) Averaged projections of the ribosome-Sec61 complex obtained by classification. Particles marked with arrowheads show the ribosome in side view, with the Sec61 complex visible as a 100 Å–long mass lying parallel to the ribosome surface. Scale bar, 200 Å.

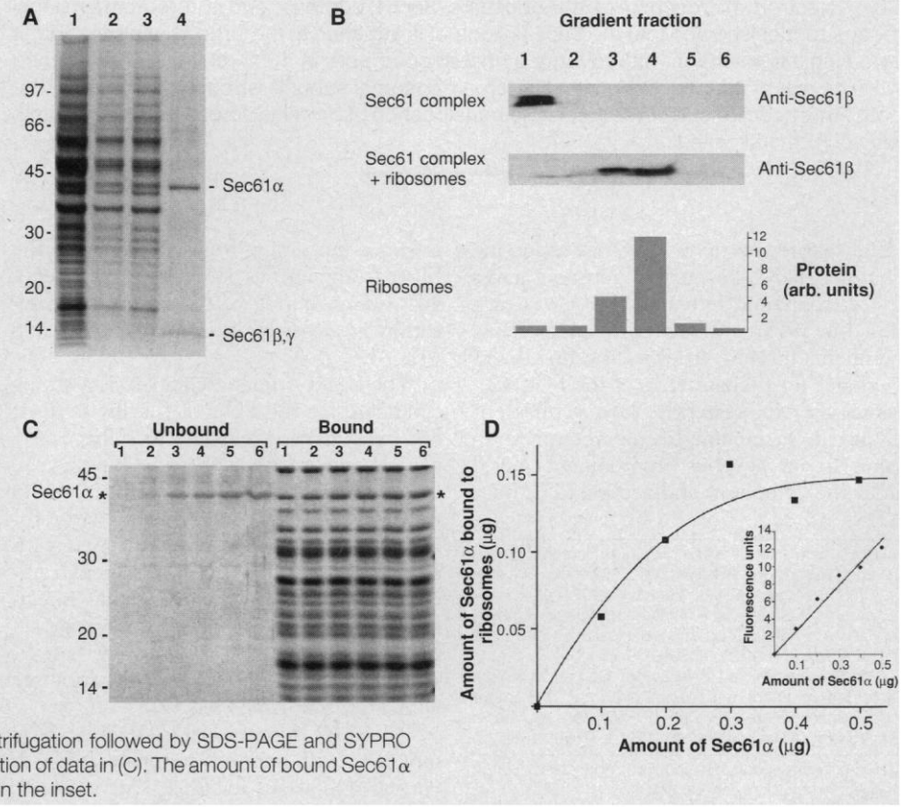

Fig. 1. Purification and binding of the trimeric Sec61 complex to ribosomes. (**A**) Purification of the Sec61 complex. Crude nuclear envelopes from *Sec63prA* cells were extracted with digitonin, and the digitonin extract was incubated with IgG-Sepharose. The trimeric Sec61 complex was eluted with Triton X-100 and analyzed by SDS-PAGE followed by Coomassie blue staining. Lane 1, crude nuclear envelopes (1/30,000); lane 2, digitonin extract (1/30,000); lane 3, IgG-Sepharose flow through (1/30,000); and lane 4, Triton X-100 eluate (1/10). Ten to 15 micrograms of Sec61α [by comparison with a bovine serum albumin standard] were typically purified from 80 g of packed cells. Molecular mass is given in kilodaltons at the left. (**B**) The Sec61 complex binds to ribosomes. The Sec61 complex (0.5 μg) was incubated with and without ribosomes (0.5 A_{260}), and the incubation mixture was analyzed by sucrose density-gradient centrifugation followed by SDS-PAGE analysis and immunoblotting of gradient fractions. Lanes 1 to 6 represent top to bottom fractions probed with a peptide antibody to Sec61β. For the ribosomes, the Coomassie-stained proteins were quantitated with NIH image (arb. units, arbitrary units). (**C**) Binding of the Sec61 complex to ribosomes is saturable. Increasing amounts of the Sec61 complex (0 μg of Sec61α in lane 1 to 0.5 μg of Sec61α in lane 6) were incubated with a fixed amount of ribosomes (0.125 A_{260}) and analyzed by density-gradient centrifugation followed by SDS-PAGE and SYPRO Red staining. Asterisks denote Sec61α. (**D**) Quantitation of data in (C). The amount of bound Sec61α was calculated according to the calibration shown in the inset.

have been proposed as exit pathways of the nascent polypeptide chain, although the evidence for that is indirect (*20*). The precise alignment between the pore of the Sec61 oligomer and the tunnel (Fig. 3, C and D) provides strong support for this hypothesis. Conversely, this structural arrangement also implies that the Sec61 oligomer indeed constitutes the PCC.

Detailed analysis of the Sec61 oligomer (Fig. 4, A to C) shows that the azimuthal distribution of mass is irregular, with the bulk of the mass lying on the side attached to the stem. Again, as speculated above, the thinner wall opposite the attachment stem might facilitate lateral opening of the channel. There is a further asymmetry in the Sec61 oligomer: the pore is funnel-shaped, with a diameter of 15 Å at the lumenal site of the ER, widening toward the ribosome, so that a small vestibule with a diameter of 35 Å is formed. Consistent with the estimate from kinetic data, the measured volume of the Sec61 oligomer would accommodate two trimeric Sec61 complexes. The reasons for the asymmetric appearance of the ribosome-bound Sec61 oligomer are presently not clear.

It is likely that the Sec 61 oligomer bound to the ribosome represents the PCC in its inactive and closed conformation. Future structural analyses of an in vitro–assembled complex containing a ribosome, a nascent chain, and the Sec61 complex will lead to information regarding the active state of the PCC.

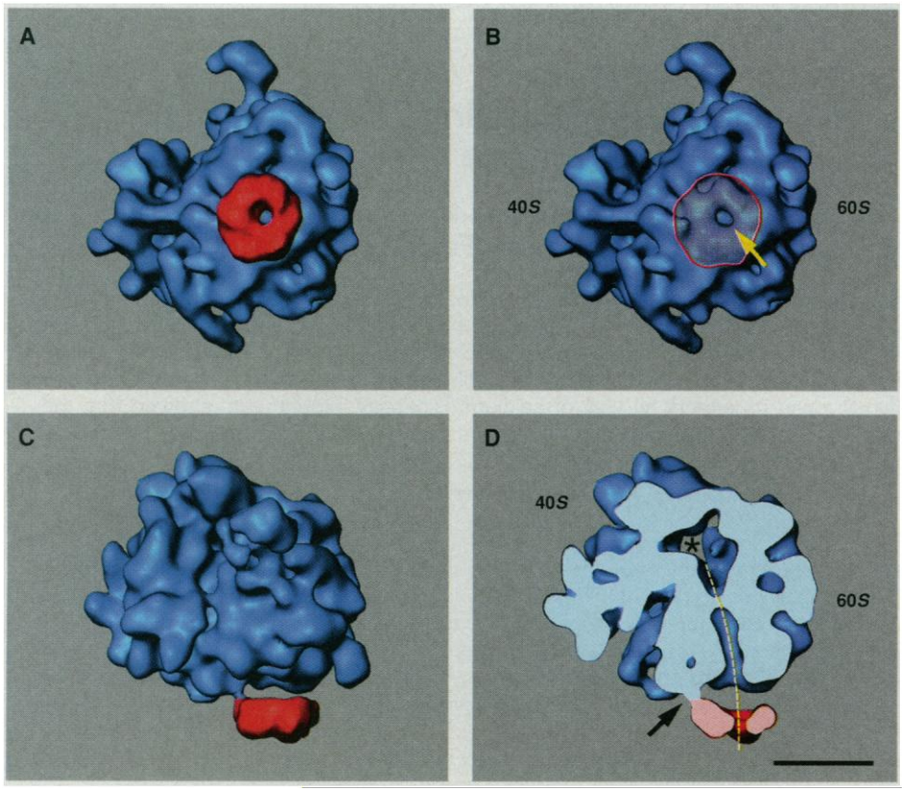

Fig. 3. Three-dimensional reconstruction of the ribosome-Sec61 complex in a surface representation. (**A**) Front view, with the Sec61 oligomer shown in red. (**B**) Front view, with the Sec61 oligomer shown as transparent, to demonstrate the alignment of the Sec61 oligomer pore with the tunnel exit of the large ribosomal subunit indicated with the yellow arrow. (**C**) Side view, with the Sec61 oligomer shown in red. (**D**) Ribosome-Sec61 complex lying in the same orientation as in (C), cut along a plane that cross sections the pore of the Sec61 oligomer and the ribosome tunnel. The arrow indicates the stem connecting the ribosome with the Sec61 oligomer; the space between the two ribosomal subunits is indicated by an asterisk. The ribosomal tunnel and its alignment with the Sec61 pore is indicated by a broken yellow line. Scale bar, 100 Å.

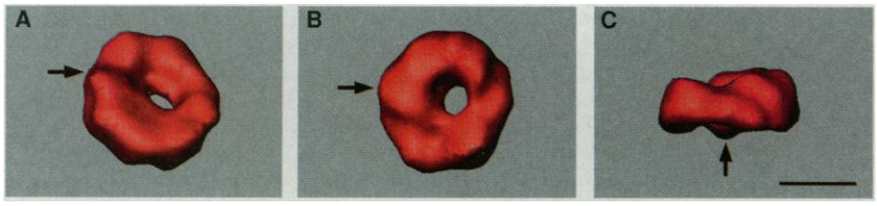

Fig. 4. Three closeup views of the Sec61 oligomer. (**A**) Surface facing the ribosome. There is a vestibule (diameter of 35 Å) formed by the funnel-like structure and the pore (diameter of 15 Å). (**B**) Surface facing away from the ribosome. (**C**) View of the side opposite the attachment site. The ribosome would be located underneath the channel. The wall opposite the attachment site is thinner and more irregular. Arrows indicate the attachment site. Scale bar, 50 Å.

REFERENCES AND NOTES

1. G. Blobel and B. Dobberstein, *J. Cell Biol.* **67**, 835 (1975).
2. S. M. Simon and G. Blobel, *Cell* **65**, 371 (1991); *ibid.* **69**, 677 (1992).
3. K. S. Crowley, G. D. Reinhart, A. E. Johnson, *ibid.* **73**, 1101 (1993); K. S. Crowley, S. Liao, V. E. Worrel, G. D. Reinhart, A. E. Johnson, *ibid.* **78**, 461 (1994).
4. B. D. Hamman, J.-C. Chen, E. E. Johnson, A. E. Johnson, *ibid.* **89**, 535 (1997).
5. R. J. Deshaies and R. Schekman, *J. Cell Biol.* **105**, 633 (1987); C. J. Stirling, J. Rothblatt, M. Hosobuchi, R. Deshaies, R. Schekman, *Mol. Biol. Cell* **3**, 129 (1992).
6. D. Görlich, S. Prehn, E. Hartmann, K. U. Kalies, T. A. Rapoport, *Cell* **71**, 489 (1992); D. Görlich and T. A. Rapoport, *ibid.* **75**, 615 (1993).
7. K. U. Kalies, D. Görlich, T. A. Rapoport, *J. Cell Biol.* **126**, 925 (1994).
8. B. Jungnickel and T. A. Rapoport, *Cell* **82**, 261 (1995).
9. D. Hanein *et al.*, *ibid.* **87**, 721 (1996).
10. J. Frank *et al.*, *Nature* **376**, 441 (1995); H. Stark *et al.*, *Structure* **3**, 815 (1995).
11. A. Verschoor, S. Srivastava, R. Grassucci, J. Frank, *J. Cell Biol.* **133**, 495 (1996).
12. A. Verschoor, J. R. Warner, S. Srivastava, R. A. Grassucci, J. Frank, *Nucleic Acids Res.*, in press.
13. A yeast strain (*Sec63prA*) was constructed in which the genomic copy of the gene encoding Sec63p was tagged by COOH-terminal, in-frame integration of a DNA fragment encoding for the immunoglobulin G (IgG)–binding domains of protein A. The DNA fragment encoding the protein A gene and adjacent *HIS3* and *URA3* markers was amplified by polymerase chain reaction with specific primers for *SEC63* and a template plasmid as described [J. D. Aitchison, M. P. Rout, M. Marelli, G. Blobel, R. Wozniak, *J. Cell Biol.* **131**, 1133 (1995)]. A crude nuclear pellet was prepared from a 36-liter culture as described (C. Strambio-de-Castillia, G. Blobel, M. P. Rout, *ibid.*, p. 19). Thirty milliliters of crude nuclei (one-fifth of the preparation) was extracted by incubation with deoxyribonuclease I (20 μg/ml) and Heparin (1 mg/ml) in buffer E [10 mM bis-tris-Cl (pH 6.5), 1 mM $MgCl_2$, 10 mM KOAc, 1 mM dithiothreitol (DTT), and 0.5 mM phenylmethylsulfonyl fluoride (PMSF)] for 20 min at 25°C and 40 min on ice. The crude nuclear envelopes were sedimented for 40 min at 145,000*g* at 4°C and extracted with 40 ml of buffer S [3% digitonin, 0.4 M sucrose, 10 mM triethanolamine-OAc (pH 7.5), 750 mM KOAc, 1.5 mM $Mg(OAc)_2$, 0.5 mM EDTA, and 1 mM DTT] for 30 min on ice. After pelleting by centrifugation of insoluble material for 35 min at 145,000*g* at 4°C, the extract was diluted with 1 volume of buffer D [0.4 M sucrose, triethanolamine-OAc (pH 7.5), 1.5 mM $Mg(OAc)_2$, 1 mM PMSF, and 1 mM DTT] and incubated overnight with 1 ml of IgG-Sepharose (Cappel, Durham, NC) at 4°C. The column was washed with 10 volumes of buffer W [1% digitonin, 100 mM KOAc, Azolectin (0.5 mg/ml), 10 mM triethanolamine-OAc (pH 7.5), 10% glycerol, 3 mM $Mg(OAc)_2$, 0.5 mM DTT, and 1 mM $CaCl_2$], and the trimeric Sec61 complex was eluted with buffer T [1% Triton X-100, 200 mM KOAc, 10 mM triethanolamine-OAc (pH 7.5), 10% glycerol, 3 mM $Mg(OAc)_2$, 0.5 mM DTT, and 1 mM $CaCl_2$]. The

identity of the proteins was confirmed by specific antibodies to Sec61α (Sec61p) and Sec61β (Sbh1p) (*17*).
14. S. Panzner, L. Dreier, E. Hartmann, S. Kostka, T. A. Rapoport, *Cell* **81**, 561 (1995)
15. For the purification of ribosomes, the yeast strain DF5 was grown in 3.5 liters of yeast extract, peptone, and dextrose medium. At an optical density of 600 nm (OD_{600}) of 1.0, the cells were washed with water and incubated for 15 min at 25°C in 100 mM tris-SO_4 (pH 9.4) and 10 mM DTT. After homogenization by French press in buffer A [50 mM triethanolamine-OAc (pH 7.5), 50 mM KOAc, 5 mM $MgCl_2$, 1 mM DTT, and 0.5 mM PMSF], the homogenate was centrifuged for 30 min at 100,000*g* at 4°C. The supernatant was layered over a continuous 10 to 40% sucrose gradient in buffer A. After centrifugation for 4.5 hours at 200,000*g* at 4°C, the monomeric ribosomes were pooled according to the A_{254} profile. The ribosomes were pelleted by centrifugation for 4.5 hours at 145,000*g* at 4°C, resuspended in water, and frozen in liquid N_2.
16. Purified Sec61 complex and ribosomes were incubated for 30 min on ice in a buffer containing 0.5% Triton X-100, 100 mM KOAc, 5 mM triethanolamine-OAc (pH 7.5), 5% glycerol, 1.5 mM $Mg(OAc)_2$, 0.5 mM DTT, and 0.5 mM $CaCl_2$. To separate unbound Sec61 complex from ribosome-bound Sec61 complex, we carried out gradient centrifugation using a 10 to 50% sucrose step gradient in 0.5% Triton X-100, 100 mM KOAc, 10 mM triethanolamine-OAc, 1 mM DTT, and 3 mM $Mg(OAc)_2$. After centrifugation for 60 min at 240,000*g* at 4°C, six fractions were collected manually. For saturation assays, the first two fractions were pooled as the unbound fraction and the following two as the bound fraction. Fractions were analyzed by SDS–polyacrylamide gel electrophoresis (PAGE) and stained with SYPRO Red. The amount of protein was quantitated with the STORM system (red fluorescence) and NIH image. For immunoblotting, proteins were precipitated, separated on 10 to 20% SDS-PAGE gradient gels, transferred to a nitrocellulose membrane, incubated consecutively with anti-Sec61α or anti-Sec61β and horseradish peroxidase–conjugated donkey antibodies to rabbit, and detected by ECL as described (Amersham).
17. R. Beckmann *et al.*, data not shown.
18. Incubation to form the ribosome-Sec61 complex was performed as described (*16*), and the mixture was diluted with 4 volumes of water immediately before it was applied to the grid. Grids for cryo–electron microscopy were prepared as described [T. Wagenknecht, R. Grassucci, J. Frank, *J. Mol. Biol.* **199**, 137 (1988); J. Dubochet *et al.*, *Q. Rev. Biophys.* **21**, 129 (1988)]. Micrographs were recorded under low-dose conditions on a Philips EM 420, with 1.5-μm defocus and magnification of 52,200 ± 2% as checked by a tobacco mosaic virus standard.
19. P. A. Penczek, R. Grassucci, J. Frank, *Ultramicroscopy* **53**, 251 (1994).
20. C. Bernabeu, E. M. Tobin, A. Fowler, I. Jabin, J. A. Lake, *J. Cell Biol.* **96**, 1471 (1983).
21. Micrographs were checked for drift, astigmatism, and presence of Thon rings by optical diffraction. Scanning was done with a step size of 25 μm corresponding to 4.78 Å on the object scale, on a Perkin-Elmer PDS 1010 A microdensitometer. Particles were selected by an automated selection procedure that differed from the one previously described [K. R. Lata, P. Penczek, J. Frank, *Ultramicroscopy* **58**, 381 (1995)] in that the particle candidates were compared directly with the reference set of 87 quasi–evenly spaced projections (*19*) of an existing reconstruction of the ribosome from yeast (*12*). A total of 13,178 particles were picked. The reconstruction was done with two independent approaches to obtain the orientations of the projections. In the first approach, an existing reconstruction of the ribosome from yeast (*12*) was used as a reference in the 3D projection alignment procedure (*19*). In the second approach, an initial reconstruction was obtained with the simultaneous minimization technique [P. Penczek, J. Zhu, J. Frank, *Ultramicroscopy* **63**, 205 (1996)]. In both cases, four steps of the 3D projection alignment procedure (*19*) were applied with a 2° angular interval. In each step, the refined 3D structure was calculated with 70% of the best matching particles (on the basis of the value of the cross-correlation coefficient). Both reconstructions proved to be indistinguishable within the measured resolution range. The final resolution, estimated with the Fourier shell correlation with a cutoff value at 0.5 [B. Böttcher, S. A. Wynne, R. A. Crowther, *Nature* **386**, 88 (1997)], was 26 Å.
22. R. Gilmore and G. Blobel, *Cell* **42**, 497 (1985).
23. In trying to gauge the correct threshold value, we were led by two criteria: (i) We observed the structure as the threshold was increased. There is normally a "plateau," a range of threshold values within which the appearance (or the volume encompassed) varies only slightly. (ii) Three-dimensional connectivity must not be violated, which means that, in this case, we could not choose a threshold, within the plateau defined above, that makes the connecting rod disappear. Thus, the plateau was further narrowed. These criteria were applied separately in the preparation of the 3D representations of the ribosome and the channel. Because of the residual uncertainty in the molecular boundaries, the measurements for pore size and the distance between channel and ribosome have an uncertainty of 25%.
24. We thank A. Fischer for the purification of the Sec61 complex; members of the Blobel lab and R. Agrawal for discussions; S. Darst and A. Malhotra for discussions, support with the electron microscopy, and assistance with the image processing; A. Heagle for help with the illustrations; and the National Center for Supercomputer Applications, University of Illinois at Urbana-Champaign, for computing support. Supported by grants from NIH (1R01 GM29169) and NSF (BIR 9219043) (to J.F.) and a fellowship of the Deutsche Foschungsgemeinschaft (to R.B.).

26 September 1997; accepted 17 November 1997

Abscisic Acid Signaling Through Cyclic ADP–Ribose in Plants

Yan Wu, Jennifer Kuzma, Eric Maréchal,* Richard Graeff, Hon Cheung Lee, Randy Foster, Nam-Hai Chua†

Abscisic acid (ABA) is the primary hormone that mediates plant responses to stresses such as cold, drought, and salinity. Single-cell microinjection experiments in tomato were used to identify possible intermediates involved in ABA signal transduction. Cyclic ADP–ribose (cADPR) was identified as a signaling molecule in the ABA response and was shown to exert its effects by way of calcium. Bioassay experiments showed that the amounts of cADPR in *Arabidopsis thaliana* plants increased in response to ABA treatment and before ABA-induced gene expression.

Plants endure environmental challenges such as drought, salinity, or cold by adjusting rather than escaping. These responses are mediated by ABA (*1*), which through unknown signals affects the regulation of many genes (*2–7*). One signaling intermediary is calcium (Ca^{2+}) (*8*). ABA-mediated increases in guard cell Ca^{2+} levels lead to stomatal closure (*9*). Ca^{2+} can also induce the expression of an ABA-responsive gene in maize protoplasts (*10*).

Three regulators of Ca^{2+} levels are inositol (1,4,5)-trisphosphate (IP_3) (*11*), cyclic adenosine 5′-diphosphate ribose (cADPR), and nicotinic acid adenine dinucleotide phosphate ($NAADP^+$) (*12–15*). The receptor for IP_3 is known (*11*), whereas those for cADPR and $NAADP^+$ are not (*15*). A putative receptor for cADPR is the ryanodine receptor (RyR) (*15*). $NAADP^+$, a metabolite of nicotinamide adenine dinucleotide phosphate ($NADP^+$) identified in vitro, regulates a third Ca^{2+} channel that appears to be distinct from the IP_3 and cADPR receptors (*14*). cADPR can be produced by ADP–ribosyl cyclase or by CD38, a lymphocyte protein, both of which use nicotinamide adenine dinucleotide (NAD^+) as a precursor (*16*).

Both IP_3 and cADPR elicit Ca^{2+} release from beet storage root vacuoles (*17*), and a RyR-like activity, sensitive to cADPR, has been detected in beet microsomes (*18*). Here we demonstrate that cADPR is a likely in vivo intermediate of ABA signal transduction that exerts its effects by way of intracellular Ca^{2+} release.

We used microinjection to screen for compounds that may be involved in ABA responses. We studied the *Arabidopsis* genes *rd29A* (also termed *Iti78* and *cor78*) (*5*), a desiccation-responsive gene (*3*), and *kin2* (also termed *cor6.6*) (*5*), a cold-inducible gene (*2*). Both genes are rapidly induced by ABA, without requiring new protein synthesis.

We microinjected 7- to 10-day-old etiolated hypocotyls of the phytochrome-deficient tomato mutant *aurea* (*19*, *20*) with *rd29A-GUS*, *kin2-GUS* (*21*), and potential agonists and antagonists of ABA signal

Y. Wu, J. Kuzma, E. Maréchal, R. Foster, N.-H. Chua, Laboratory of Plant Molecular Biology, Rockefeller University, 1230 York Avenue, New York, NY 10021–6399, USA.
R. Graeff and H. C. Lee, Department of Physiology, University of Minnesota, Minneapolis, MN 55455, USA.

*Present address: Laboratoire de Physiologie Cellulaire Végétale, Departement de Biologie Moleculaire et Cellulaire, Universite Joseph Fourier et CEA-Grenoble, 17 rue des Martyrs, F-38054 Grenoble Cedex 9, France.
†To whom correspondence should be addressed. E-mail: chua@rockvax.rockefeller.edu